A Mathematical Model of the Moisture Gradient in Air-Dried Square Heavy Timbers of Japanese Red Pine

Kang, Chun-Won
Department of Housing Environmental Design, and Research Institute of Human Ecology, College of Human Ecology, Chonbuk National University

Lee, Yong Hun
Department of Mathematics, College of Natural Science, Chonbuk National University

Kang, Ho-Yang
Department of Bio-based Materials, Chungnam National University

Kang, Seog-Goo
Department of Bio-based Materials, Chungnam National University

他

https://doi.org/10.5109/1543407

出版情報：九州大学大学院農学研究院紀要. 60 (2), pp.445-450, 2015-09-18. Faculty of Agriculture, Kyushu University
バージョン：
権利関係：

J. Fac. Agr., Kyushu Univ., **60** (2), 445–450 (2015)

A Mathematical Model of the Moisture Gradient in Air–Dried Square Heavy Timbers of Japanese Red Pine

Chun–Won KANG[1], Yong Hun LEE[2]*, Ho–Yang KANG[3], Seog–Goo KANG[3], Ik–Hyun SHIN[4] and Noboru FUJIMOTO

Laboratory of Wood Material Technology, Division of Sustainable Bioresources Science,
Department of Agro–environmental Sciences, Faculty of Agriculture,
Kyushu University, Fukuoka 812–8581, Japan
(*Received May 8, 2015 and accepted May 19, 2015*)

Moisture content variation along the thickness direction of square heavy timbers of Japanese red pine (20 × 20–cm cross–section, 360 cm length) of a control and those kerfed in the longitudinal direction were mathematically simulated during air drying. The model was based on anatomical features, and the heat and mass transfer of the wood.

The model was solved numerically in order to predict the moisture content profiles. Then, the estimated moisture content variation was compared to that of the experimental value of the square heavy timbers.

The square heavy timbers were dried to a moisture content of 14% for the kerfed and 15% for the control wood. The final moisture content differences between the internal and external layers of the kerfed and control wood specimens were 2% and 2.5%, respectively. The moisture gradient in the thickness direction was very smooth. The moisture content variance in the thickness direction with kerfing was almost same to that of the control.

The mathematically estimated moisture gradient was in good agreement with the experimentally evaluated values.

Key words: Air drying, Longitudinal kerfing, Moisture content gradient, Mathematical simulation

INTRODUCTION

Wood is a hygroscopic material of which the dimensions change due to humid environments. It is also vulnerable to mold and other fungi infestations. Therefore, wood is commonly dried using several methods, such as air drying, conventional kiln drying and high temperature drying. Conventional air drying consists of the evaporation of water from the surface of the wood, and involves air circulation at atmospheric temperatures and humidity conditions.

The drying of heavy timber to be used as wooden building material is very difficult, because of its slow moisture transportation rate in the radial and tangential directions. In addition, when heavy timbers containing pith or juvenile wood are dried, severe surface checks can occur due to the drying stress between the moisture evaporating wood surface and the inner layer of wood containing liquid water. These severe drying defects and long drying times cause many problems, such as extending wooden building construction costs, decreasing external appearance, reducing strength, and decreasing insulation and durability. Therefore, it is very important that heavy timber for wooden building construction is dried with as little drying stress as possible. It is necessary to estimate an exact moisture gradient of the wood in the thickness direction, since this may allow for the adoption of a method for the reduction of the drying defects and drying time. In addition, the estimation of the moisture content gradient of the timber caused by changes in air conditions minimizes drying stress, residual moisture and dimensional changes. However, it is very difficult to estimate the moisture gradient of heavy timber during air drying because of its heavy weight and unstable moisture content variance.

On the other hand, pretreatment such as longitudinal kerfing can improve the drying speed in air drying and decrease drying defects, such as internal and surface checking. Lee *et al*., reported that the radio–frequency/vacuum drying rate increased and the drying defects decreased with longitudinal kerfing (1994: Lee and Luo, 2002: Li and Lee, 2004).

We investigated the numerical technique used to simulate the process of wood drying via computer programming. In other words, we sought to obtain the results of wood drying via computer simulation without the drying of real wood. We performed this simulation in order to determine the appropriate mathematical model. A mathematical model consists of a governing equation and some boundary conditions. The governing equations in our study represented the transfer of the moisture content and the heat used in the process of drying in the inner part of the wood, and the boundary conditions determined the amount of evaporation and absorption on the

[1] Department of Housing Environmental Design, and Research Institute of Human Ecology, College of Human Ecology, Chonbuk National University, Jeonju 561–756, Korea
[2] Department of Mathematics, College of Natural Science, Chonbuk National University, Jeonju 561–756, Korea
[3] Department of Bio–based Materials, Chungnam National University, Daejeon 305–764, Korea
[4] Course of Sustainable Bioresources Science, Department of Agro–environmental Sciences, Faculty of Agriculture, Kyushu University, Fukuoka 812–8581, Japan
* Corresponding author : (E–mail: lyh229@jbnu.ac.kr)

surface of the wood.

Research on mathematical modeling of wood drying was conducted by Whitaker (Whitaker, 1977). He proposed the volume averaging technique in order to derive a system of conservation equations for the mass, energy and momentum using the three phases (gas, liquid, and solid). Based on Whitaker's theory, many authors (Stanish *et al*., 1986; Avramidis *et al*., 1992; Turner and Perre, 1996; Pang 1997) developed mathematical modeling. Among these authors, Turner and Perre suggested a strategy for solving the system of transport equations using the control volume finite element method (CVFEM). The CVFEM is very difficult to implement, but it provides an advantage in that it ensures the conservation of mass and enthalpy through the boundary of each control volume as well as the entire domain.

In this study, we estimated the moisture content variation in the thickness direction of the control and the longitudinal kerfing treated heavy timber by air drying in order to estimate the possibility of the mathematical simulation of the moisture gradient in the thickness direction of the square heavy timber and in order to clarify the effects of longitudinal kerfing on the air drying of heavy timber. In addition, we mathematically predicted the moisture content variation in the thickness direction and compared this value to the estimated value. From these results, the predicted and estimated moisture variation in the thickness direction of large, square timber was compared, and the influence of the longitudinal kerfing treatment was discussed.

MATERIALS AND METHODS

Sample specimens

The domestic Japanese red pine (*Pinus densiflora* S. et. Z) sample was cut with a prismatic shape of approximate dimensions of 20 (radial) × 20 (tangential) × 360 (length) cm. Ten of these timbers were used for air drying (AD). Half of the timbers were used with kerfing treatment and the others were used for the control. The kerfing treatment on the surface of the wood specimens was applied by cutting the sample with a circular saw parallel to the grain. The kerfing width was 3 mm and the depth was 50 mm in each of the specimens.

Air drying

Five kerfed specimens and five non–kerfed specimens were dried by air drying. Before air drying, both the kerfed and non–kerfed heavy timbers were treated with high temperatures and low humidity in a dry kiln for 72 hours. The initial moisture content variation among the sample specimens may have been equalized by the

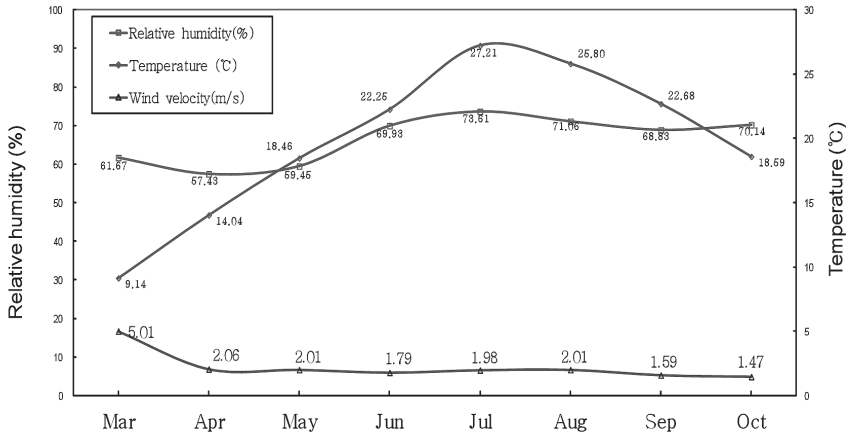

Fig. 1. Weather data from May to October as measured in Jeonju, Korea.

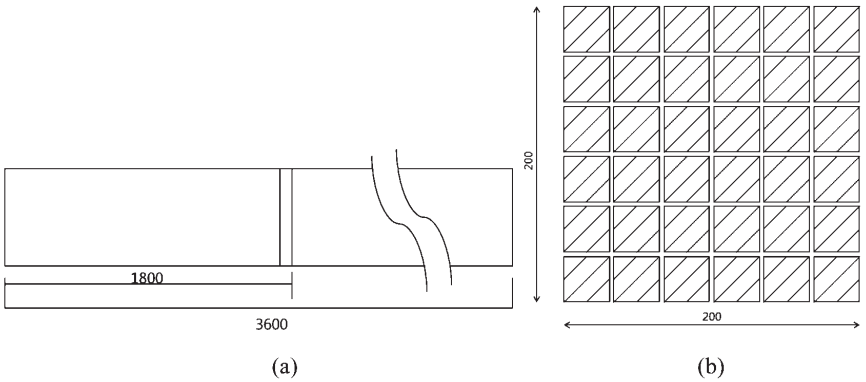

Fig. 2. Sawing diagram of the specimens for the final moisture content distribution: (a), longitu.dinal direction and (b), cross section (unit: mm).

HTLH pre–treatment. Then, the kerfed and control specimens were air dried. In this study, the initial moisture content of the kerfed and control specimens after the HTLH treatment were approximately 16% and 18%, respectively. During the air drying period from March 17, 2008 to October 7, 2008, the mean temperature was 19.8°C, the average relative humidity was 66.5%, and the mean wind velocity was 2.2 m/sec. The monthly weather conditions for March to October are presented in Fig. 1.

Drying characteristics

The moisture content and the drying rate were obtained from each of the control and treated specimens, and the weights of these samples were measured once a week. After air drying, the oven–dry weights were calculated from the final moisture contents of the specimens. For all of the samples, the moisture content of each sample was obtained in grams.

The moisture content distribution of the specimens was estimated at the point described in Figure 2a after the end of the drying period. The specimens were sawn from the sampled specimens and analyzed for final MC as shown in Fig. 2b.

Moisture gradient prediction by numerical simulation

In order to simulate the process of the wood drying numerically, we used coupled moisture–temperature model equations with the two state variables of moisture content (X) and temperature (T) (Whitaker, Perre and Turner, Kang *et al.*, 2008). The governing equations for the process of wood drying are given as follows:
Liquid Mass Conservation:

$$\frac{\partial}{\partial t}\left(\rho_o X + \varepsilon_g \rho_v\right) = \nabla \cdot J_w \text{ and}$$

Energy Conservation:

$$\frac{\partial}{\partial t}\left(\rho_o (X h_w + h_s) + \varepsilon_g (\rho_v h_v + \rho_a h_a)\right) = \nabla \cdot J_e,$$

where the fluxes J_w and J_e of the bounded water and energy are:

$$J_w = -\rho_w \bar{v}_w - \rho_v \bar{v}_g + \rho_o \bar{D}_b \nabla X_b + \rho_g \bar{D}_v \nabla \omega_v$$

and

$$J_e = -\rho_w h_w \bar{v}_w - (\rho_v h_v + \rho_a h_a)\bar{v}_g + h_b \rho_o \bar{D}_b \nabla X_b + \rho_g \bar{D}_v (h_v \nabla \omega_v + h_a \nabla \omega_a) + \bar{K}_{eff} \nabla T,$$

respectively.

The primary variables in the model equations were the moisture content X, the moisture content of the bounded water X_b, and the temperature T in Kelvin. In addition, the secondary variables and the parameters were as follows: ρ_o denoted the wood density, ρ_w the liquid water density, ρ_v the water vapor density, ρ_a the liquid air density, ρ_g the gas density, $\bar{D}_b$ the diffusion coefficient of the bound water (m^2/s) and $\bar{D}_v$ the bulk binary diffusivity of the water vapor (m^2/s). The notations of the enthalpies were h_b for the bound water, h_w for the water, h_v for the water vapor, h_a for the liquid air, and h_s for the solid water vapor (J/kg). The mass fraction of the water vapor and liquid air were denoted by ω_v and ω_a, respectively, and the gaseous volume fraction was denoted by ε_g. The liquid and gaseous phase velocities $\bar{v}_w$ and $\bar{v}_g$, respectively, could be expressed by Darcy's law. The effective thermal conductivity was denoted by $\bar{K}_{eff}$ (W/m K).

In this numerical simulation, we only considered the 2–dimensional rectangular region R'=[–0.1, 0.1] x [0.0, 0.2] (m x m), which was a flat board cut from the specimen, by neglecting the longitudinal direction effect. At the boundary surface, the moisture was evaporated in the air drying conditions, and then the moisture content and temperature were affected by the relative humidity, temperature and wind velocity of the air weather. However, as a result of the symmetry, the computational domain only used the right–half region, i.e., R=[0.0, 0.1] x [0.0, 0.2]. For the non–kerfed specimen, the full surface at x=0.0 was the symmetrical surface. On the other hand, for the kerfed specimen, only half of the surface at x=0.0, i.e., $0.0<y<0.14$, was the symmetrical surface.

The boundary conditions at the symmetrical surfaces can be given as follows:

$$-J_w \cdot n = 0 \text{ and}$$

$$-J_e \cdot n = 0.$$

In addition, the boundary conditions at the external drying surfaces can be given as follows:

$$-J_w \cdot n = h_c\left(\rho_{v,\infty} - \rho_{v,s}\right) \text{ and}$$

$$-J_e \cdot n = h_T (T_s - T_\infty) + h_c \Delta h_v \rho_{v,s} - \left(\rho_{v,s} - \rho_{v,\infty}\right),$$

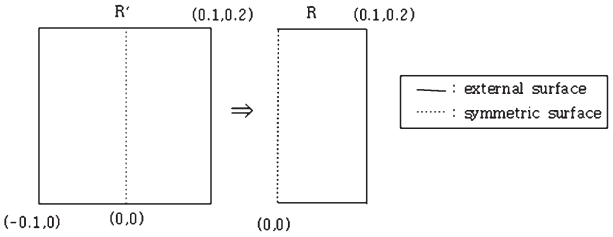

Fig. 3. Computational domain rational unit: on specimens for measual surfaces for the non–kerfed specimen.

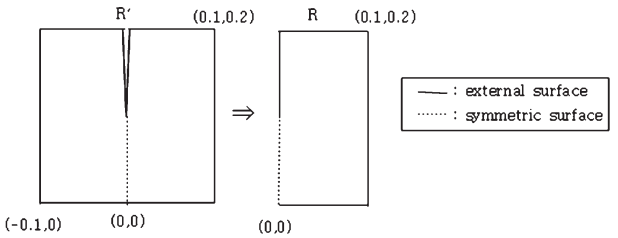

Fig. 4. Computational domain rational unit: on specimens for measual surfaces for the kerfed specimen.

where h_c and h_T are the external convective mass and the heat transfer coefficients, respectively, $\rho_{v,s}$ and $\rho_{v,\infty}$ are the water vapor density at the wood surface and of the surrounding air, respectively, T_s and T_∞ are the temperature at the wood surface and of the surrounding air, respectively, and Δ_{hv} is the latent heat of evaporation. In this study, T_∞, $\rho_{v,\infty}$ and Δ_{hv} fluctuated by the temperature, the relative humidity and the wind velocity of the air weather. Then, in this simulation, these coefficient values were calculated using the weather data, which was measured from March 17, 2008 to October 7, 2008 at Jeonju (Fig. 1).

In order to obtain the computational results for the moisture content distribution, we applied the control volume finite element methods as the discretization method. This numerical scheme is an appropriate method for the heat and mass transfer equation. As for the numerical results, we found the distribution of the moisture content and the temperature on the final day of the experiment, October 7, 2008.

RESULTS AND DISCUSSION

Drying rate and final moisture content

The relationship between the drying time and moisture content of the kerfed and control specimens in air drying are shown in Figure 5.

The initial moisture content of the kerfed and control specimens were approximately 70% and 57%, respectively. These kerfed and non–kerfed specimens were dried to approximately 16% and 18%, respectively, after 4 days of the HT–LH treatment. Therefore, the decrease in the moisture by the air drying was less than approximately 3%. During the HT–LH treatment, the drying rates of the kerfed and non–kerfed specimens were 13%/day and 9%/day, respectively. After 154 days of the air drying, the moisture contents of the kerfed and non–kerfed specimens were 14% and 15%, respectively, as shown in Figure 5.

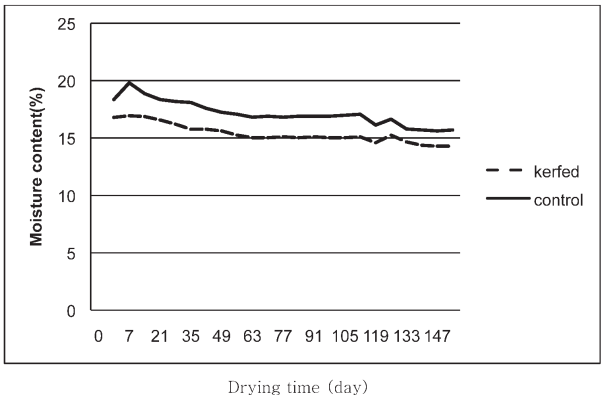

Fig. 5. The change in the MC as a function of the drying time during air drying.

12.8 *12.3*	14.1 *13.7*	14.4 *13.8*	13.0 *14.2*	14.2 *14.0*	12.9 *12.4*
13.9 *14.0*	17.2 *17.4*	17.1 *17.6*	16.9	16.8 *16.1*	14.0 *13.3*
13.2 *13.6*	17.0 *17.4*	17.8 *18.0*	17.7 *17.7*	17.0 *16.1*	14.3 *13.0*
13.7 *14.1*	17.1 *17.8*	17.4 *17.8*	17.4 *17.6*	17.1 *16.0*	14.1 *13.0*
13.3 *14.3*	16.6 *17.7*	16.7 *17.7*	16.5 *17.3*	16.1 *15.8*	13.5 *12.7*
12.1 *12.3*	12.7 *14.1*	13.4 *13.8*	13.9 *13.5*	13.2 *13.6*	11.8 *11.3*

(a)

13.6 *13.5*	14.3 *13.9*	14.6 *13.6*	14.6 *13.6*	14.3 *13.9*	13.6 *13.5*
14.3 *14.1*	16.1 *15.3*	16.9 *15.0*	16.9 *15.0*	16.1 *15.3*	14.3 *14.1*
14.6 *14.4*	16.9 *16.3*	17.7 *16.9*	17.7 *16.9*	16.9 *16.3*	14.6 *14.4*
14.6 *14.5*	16.9 *16.6*	17.9 *17.4*	17.9 *17.4*	16.9 *16.6*	14.6 *14.5*
14.3 *14.2*	16.1 *15.9*	16.9 *16.7*	16.9 *16.7*	16.1 *15.9*	14.3 *14.2*
13.6 *13.6*	14.3 *14.2*	14.6 *14.6*	14.6 *14.6*	14.3 *14.2*	13.6 *13.6*

(b)

Fig. 6. The final moisture content distribution of the specimens after air drying: (a) experimental data, (b) numerical data (Italics for kerfed treatment, common type for non–kerfed).

In view of the distribution of the final moisture content, the distribution of the moisture content in the thickness directions after drying is shown in Fig. 6. The surface MC was higher than that of the inner layer of the wood on each of the control and kerfed specimens, and the MC of the intermediate layer was almost the same or slightly higher than that of the surface layer. For easy comparison, the measured and estimated final MC distributions in the control and kerfed sample specimens are shown in Figure 6. In Fig. 5, the entire final MC of the control sample specimens was 2% higher than that of the kerfed sample specimens during air drying. The minute moisture content distribution differences are as shown in Fig. 6. In Fig. 6–a, the water content near the kerfed area is lower than that of the control specimen, but the moisture content of the kerfed sample is a little higher than that of the control specimen in other areas. This result indicated that the kerfing treatment was effective for not only lowering the MC distribution difference, but also lowering the MC of the entire sample specimen. On the other hand, in Figure 6–b, which shows the simulated MC distribution map, the moisture content of each of the kerfed specimen was lower than that of the control specimen.

Comparison between the calculated and evaluated final moisture content distribution

A mathematical model was developed in order to simulate the moisture gradient in the thickness direction of heavy timber from Japanese red pine during air drying with a moisture content value of below 20%. Therefore, it was assumed that liquid water flow did not occur in the wood, because the air drying was started after 3 days of HTLT treatment. The numerical simulation was adopted in order to predict the moisture gradient in the thickness direction in heavy timber during drying. The model was based on the heat and mass transfer in wood. The moisture content profiles from the mathematical model were calculated and the results are illustrated in Figs. 7 and 8. Their contour images show the variations in the moisture gradient along the thickness. Figure 7 shows the normal moisture gradient in the thickness direction of the air dried wood. In addition, Fig. 8 shows the normal moisture gradient in the thickness direction of the air dried wood. The calculated map also accurately indicates that the surface of the kerfed area was exposed to the air and balanced with ambient air conditions. From these results, it is possible to estimate the drying time and moisture gradient in various drying conditions, such as ambient air conditions, kerfing and sample thickness.

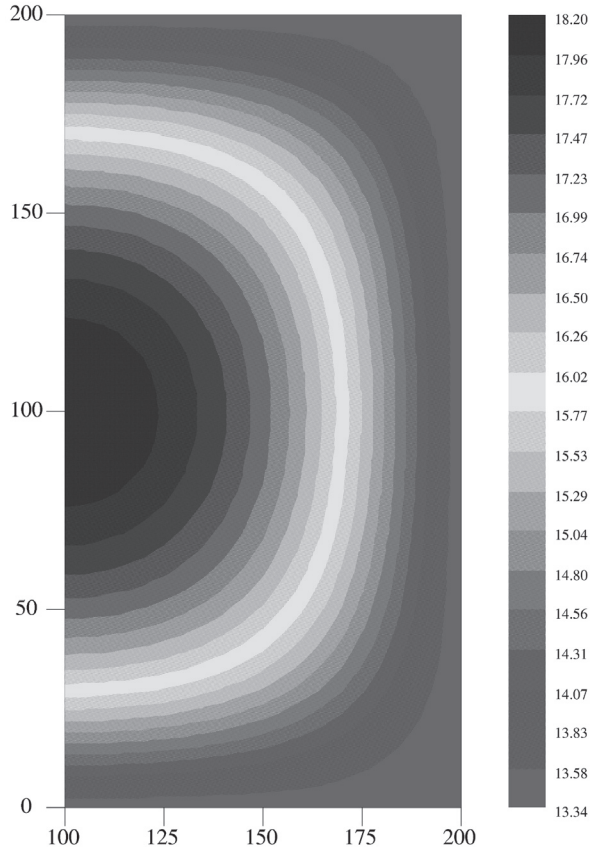

Fig. 7. Moisture gradient map of the control wood in the thickness direction by mathematical simulation.

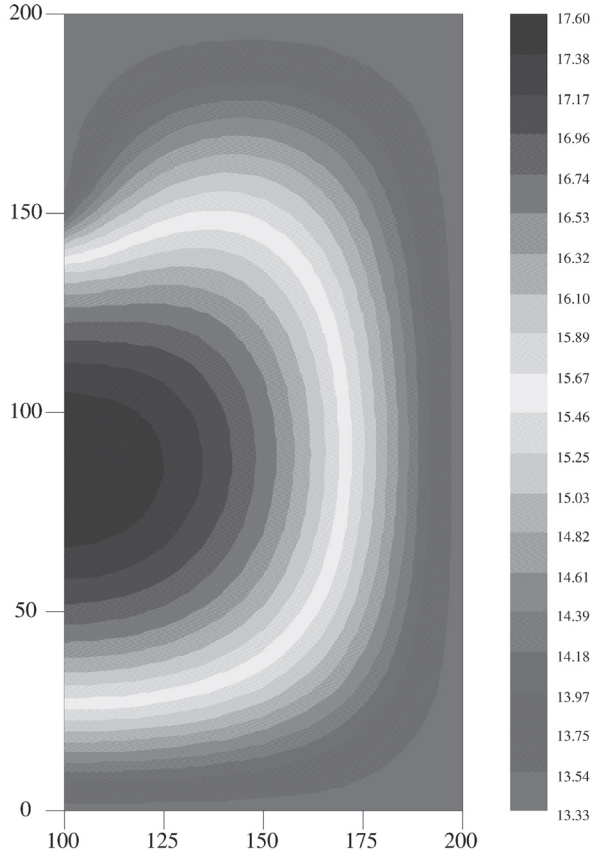

Fig. 8. Moisture gradient map of the kerfed wood in the thickness direction by mathematical simulation.

The predicted moisture content gradients were compared with the experimentally estimated data shown in Figs. 9 and 10. The average and maximum values of the moisture content difference between the kerfed and control specimens were 0.03% and 0.2%, respectively, in the case of experimental estimation. On the other hand, the average and maximum values of the moisture content difference between the kerfed and control specimens were 0.42% and 0.5%, respectively, in the case of the simulation. From these results, it can be concluded that the predicted moisture content gradient was in reasonable agreement with the measured values. The predicted moisture content gradients for the 1,800 mm of the sample specimen showed a very close trend to those of the measured data, in both the cases of the control and the kerfed specimens.

Figure 11 shows the high regression between the predicted and estimated moisture content in the thickness direction on both the kerfed and control wood specimens.

The simulation model was found to be effective for the estimation of final moisture content distribution in the

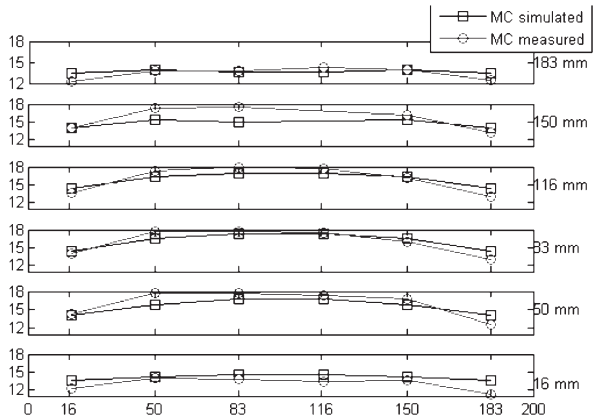

Fig. 9. Comparison between the predicted and estimated moisture gradient maps of the control Japanese red pine heavy timbers in the thickness direction.

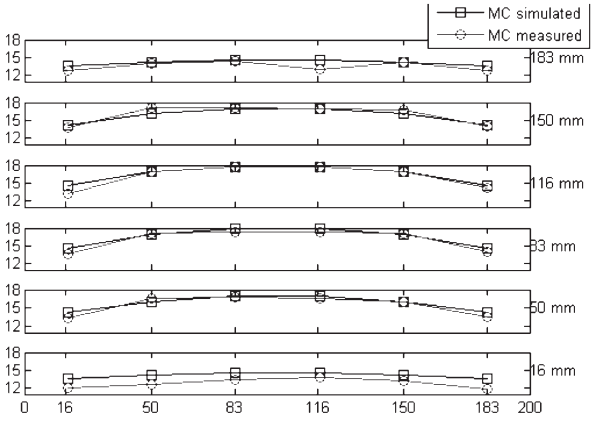

Fig. 10. Comparison between the predicted and estimated moisture gradient maps of longitudinal kerfing-treated Japanese red pine heavy timbers in the thickness direction.

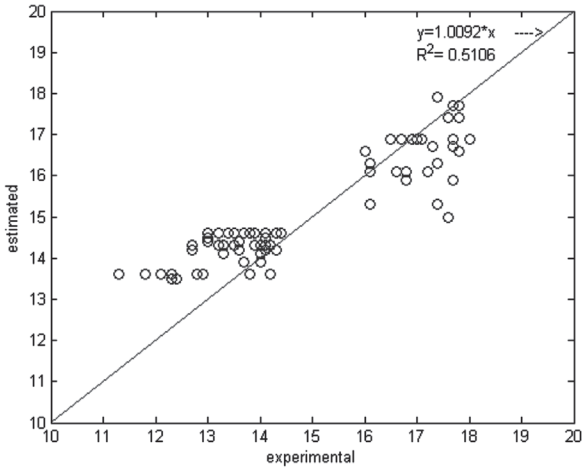

Fig. 11. Comparison between the predicted and estimated final moisture content distribution.

thickness direction because the difference between the measured and mathematically predicted values was relatively small.

CONCLUSIONS

Mathematical simulation of the moisture gradient in square heavy timbers with air drying was performed in the wood of domestic Japanese red pine boxed timbers. Air drying was adopted and the effects of longitudinal kerfing treatment on the drying characteristics were estimated. The results are summarized as follows:

The drying rates were influenced by longitudinal kerfing treatment, such that the drying time from green to 5% moisture content for the treated sample was faster than that for the control wood. Kerfing treatment of lumber was more effective than no treatment in view of the prevention of surface checking; and internal checking did not occur in the domestic Japanese red pine whether or not it was treated.

The predicted moisture gradient map was in good agreement with the estimated one.

REFERENCES

Avramidis S., Englezos P., Papathanasiou T. 1992, Dynamic nonisothermal transport in hygroscopic porous media : moisture diffusion in wood. *AIChE Journal*. **38**(8): 1279–1287

Jung Hee Suk, Kang Wook, Lee Chul Hyun. 2002. Comparison of Drying Characteristics of Square Timber by Heated Platen and Radio – frequency / Vacuum Drying. *Wood science and technology*. **30**(2): 108–114

Lee, N. H., Hayashi, K., and Jung, H. S. 1998. Effect of radio–frequency/vacuum drying and mechanical press–drying on shrinkage and checking of walnut log cross sections. Forest Products J. **48**(5): 73 –79

Lee, N. H. and Hayashi, K., 2000. Effect of end covering and low pressure steam explosion treatment on drying rate and checking during radio–frequency/vacuum drying of Japanese cedar log cross sections. J. of Solid wood products. **50**(2): 73 –78

Lee, N. H. and Luo, J. Y. 2002. Effect of steam explosion treatments on drying rates and moisture distributions during radio–frequency/vacuum drying of larch pillar combined with a longitudinal kerf. J. of Wood Science. **48**: 270–276

Li, C. Y. and Lee, N. H. 2004. Effect of compressive load on shrinkage of larch blocks during radio–frequency vacuum heating. *Wood and Fiber Science*. **36**(1): 9–16

Pang S. 1996. Moisture content gradient in a softwood board during drying: simulation from 2–D model and measurement. *Wood Science and Technology*. **30**: 165–178

Pang S. 1997. Relationship between a diffusion model and a transport model for softwood drying. *Wood and Fiber Science*. **29**(1): 58–67

Perre P., Moser M., Martin M. 1993. Advances in transport phenomena during convective drying with superheated steam and moist air. *Int J Heat Mass Transfer*. **36**(11):2725–2746

Stanish A., Schajer S., Kayihan F. 1986, A mathematical model of drying for hygroscopic porous media. AIChE Journal. **32**(8): 1301–1311

Turner I. W. and P. Perre 1996, A synopsis of the strategies and efficient resolution techniques used for modeling and numerically simulating the drying process, Mathematical Modeling and Numerical Techniques in Drying Technology, New York: 1–82

Whitaker S. 1977. Simultaneous heat, mass and momentum transfer in porous media: A theory of drying, *Advances in Heat Transfer* **13**: 119–203